NJC

Accepted Manuscript

This is an *Accepted Manuscript*, which has been through the Royal Society of Chemistry peer review process and has been accepted for publication.

Accepted Manuscripts are published online shortly after acceptance, before technical editing, formatting and proof reading. Using this free service, authors can make their results available to the community, in citable form, before we publish the edited article. We will replace this *Accepted Manuscript* with the edited and formatted *Advance Article* as soon as it is available.

You can find more information about *Accepted Manuscripts* in the Information for Authors.

Please note that technical editing may introduce minor changes to the text and/or graphics, which may alter content. The journal's standard Terms & Conditions and the Ethical guidelines still apply. In no event shall the Royal Society of Chemistry be held responsible for any errors or omissions in this *Accepted Manuscript* or any consequences arising from the use of any information it contains.

ROYAL SOCIETY OF CHEMISTRY

www.rsc.org/njc

Gas phase hydrogenation of levulinic acid to γ-valerolactone over supported Ni catalysts with formic acid as hydrogen source

Varkolu Mohan[1]*, Velpula Venkateshwarlu, Burri David Raju, Kamaraju Seetha Rama Rao *

*Inorganic & Physical Chemistry Division, Indian Institute of Chemical Technology, Hyderabad-500607, India. Tel.: +91 40 27191712; Fax: +91 40 27160921,

E-mail:ksramarao@iict.res.in.

[1] Present address: School of Chemistry & Physics, University of KwaZulu-Natal, Westville Campus, Chiltern Hills, Durban-4000, South Africa. E-mail:mohan.iict@gmail.com, Varkolum@ukzn.ac.za.

Abstract

The catalytic continuous vapor phase hydrogenation of levulinic acid (P = 1 atm; T = 250 °C) in the absence of external hydrogen was investigated over inorganic oxide (Al_2O_3, MgO and Hydrotalcite) supported Ni (30 wt%) catalysts. The present protocol enables the utilization of unavoidable co-product (i.e. formic acid) formed during the production of levulinic acid as a hydrogen source. Among the tested catalysts, Ni/Al_2O_3 catalyst to be an efficient catalyst for the production of γ–valerlactone through the hydrogen independent hydrogenation. The significant decrease in catalytic performance of Ni/MgO and Ni/Hydrotalcite catalysts were observed during the time on stream; while a gradual decrease was noticed in the catalytic performance of Ni/Al_2O_3 catalyst. The considerable decline in catalytic performance of Ni/MgO and Ni/Hydrotalcite catalysts were attributed to the water generation during the course of the reaction rather than the coking of reaction intermediates (angelica lactone). Furthermore, the co-feeding of water and formic acid with levulinic acid was performed and noticed the significant decrease in the catalytic performance of Ni/MgO and Ni/Hydrotalcite catalysts compare to Ni/Al_2O_3 catalyst. The results evidently signify the role of water on the activity of Ni/MgO and Ni/Hydrotalcite catalysts which could be ascribed to brucite – periclase transition of MgO with the water, which formed during the hydrogenation of levulinic acid.

Keywords: vapour phase, hydrogenation, levulinic acid, formic acid, Ni/Al_2O_3

Introduction

With the growing anxiety about environmental pollution and ever rising rigorous energy demand. A sustainable progress is necessary owing to the energy exhaust and global warming. The imbalance was created due to rapid depletion of exhaustible fuels through the anthropogenic actions than its generation. Furthermore, utilizations of these limited fuels discharge carbon dioxide (CO_2) to the environment. To tackle the problems associated with the exhaustible fuels, we need to explore for an alternative source. In this scenario, leading researchers from the globe have predicted the "Roadmap for Biomass Technologies" due to its vast availability and expected to produce 20% of fuels and 25% of chemicals. Additionally, biomass is the fourth most abundant source available on the globe after coal, natural gas, and crude oil. Currently, 14% of biomass being used for energy supply and rest of the biomass is useless [1]. So, the utilization of biomass and/or biomass-derived platform molecules to fuels, fuel additives, and chemicals are crucial.

Consequently, utilization of biomass burgeoning lot of interest due to deteriorating of fossil fuels and a global warming effect on the environment. Production of fuels and chemicals from the biomass composed of two steps: 1) production of small intermediates 2) further to fuels and chemicals from the intermediate. One such intermediate is the levulinic acid which is generally obtained by the hydrolysis of cellulose, furfuryl alcohol and also a by-product of the paper industry [2]. Hydrogenation of levulinic acid, which consists of both -C=O and –COOH can give γ-valerolactone (GVL), 2-methyl tetrahydrofuran (2MeTHF), and 1, 4-Pentanediol respectively from the subsequent hydrogenation. In particular, GVL has a lot of applications such as the solvent for lacquers, insecticides, and adhesives, in cutting oil, brake fluid and coupling agent in dye bath [3], along with these applications, we can also produce fuels and chemicals from this chemical such as diesel fuel and jet fuels [4-6].

The production of GVL from the hydrogenation of LA can be done by both homogeneous and heterogeneous catalytic systems [7]. In the literature, it is reported that the hydrogenation of levulinic acid can be done in the batch as well as the continuous process [7]. The continuous process has several advantages like ease of product separation, solvent-free conditions, etc. In turn, hydrogenation is possible in both the ways either by using molecular hydrogen or utilization of formic acid as a sole hydrogen source. Formic acid comprised of 4.4 wt % hydrogen storage, in addition, it can release stored hydrogen by heterogeneous catalysts and also nowadays its utilization as an immense interest because of

its state-of-the-art of storage capacity and also its production through simple biomass processing. In our previous works, we performed the levulinic acid hydrogenation using molecular hydrogen over Ni-based catalysts [2, 8 -12]. Besides, we also shown the influence of impurities like formic acid and water on the hydrogenation activity [8, 10]. The earlier works made us to show interest in the hydrogenation of levulinic acid in the absence of an external hydrogen (H_2) or use of formic acid as a hydrogen source. It is noteworthy to mention that the Ni-based catalysts are efficient for the dehydrogenation of formic acid [13-16]. Furthermore, the Shell oil company patented the hydrogenation of levulinic acid and its esters using formic acid as a sole hydrogen source [17]. Few researchers reported the hydrogen independent hydrogenation of levulinic acid [18, 19]. Recently, few studies suggested the hydrogenation of levulinic acid using formic acid as hydrogen source [12, 20]. In particular, formic acid has diverse benefits, for example, renewable nature, inexpensive and safer than gaseous hydrogen derived from petroleum derivatives. On the other hand, formic acid decomposes to H_2 and CO_2, the in situ liberated H_2 more reactive than the ex situ H_2.

Hence, the present work focused on the preparation of Ni-based catalysts and their evaluation for levulinic acid hydrogenation in the absence of an external hydrogen (H_2) or utilization of formic acid as a sole hydrogen source. The extensive physicochemical characterization of the catalysts were done by means of XRD, SEM, TEM-SAED, HRTEM, N_2 physisorption analysis, H_2-TPR and H_2 pulse chemisorption techniques (see supplementary information). The prepared catalysts, namely, Ni/Al_2O_3, Ni/MgO, and Ni/HT were designated as NA, NM and NHT respectively hereafter and applied to gas phase hydrogenation of biomass-derived levulinic acid to γ- valerolactone with formic acid as sole hydrogen source at 250 °C at atmospheric pressure.

Experimental

Materials and catalysts preparation

Materials $Ni(NO_3)_2$ $6H_2O$ (M/s. LOBA Chemie, India, 98%); commercial supports such as Al_2O_3 (M/s. Sud-Chemie, India), MgO (M/s.Sd fine India Ltd, India) were purchased and used without any further purification. The Mg-Al hydrotalcite (Mg/Al=2) support was prepared by precipitation method reported elsewhere [21, 22]. In a typical synthesis, nitrate

precursors of the Mg and Al were dissolved in deionized water and precipitated by 5% NaOH and 5% Na_2CO_3 mixed solution by maintaining the pH in a range of 9-12. The resulting precipitate was filtered and washed thoroughly with deionized water several times till the excess base was removed. Subsequently, the filtered mass was dried overnight in an air oven and then calcined at 450 °C for 18 h. Al_2O_3, MgO and Hydrotalcite supported Ni catalysts were prepared by conventional wet impregnation method by adding the inorganic oxide support to a $Ni(NO_3)_2 \cdot 6H_2O$ (M/s. Sd fine India Ltd, India) aqueous solutions followed by drying at 80 °C until dryness, the amount of Ni loading was fixed at 30 wt %. The resultant solids were dried at 100 °C for 12 h and, then, calcined in air at 450 °C for 5 h. The prepared catalysts Ni/ Al_2O_3, Ni/MgO and Ni/ MgO-Al_2O_3 are designated as NA, NM and NHT respectively.

Catalyst Characterization:

XRD patterns of the catalysts were registered using a Rigaku Ultima-IV (M/s Rigaku Corporation, Japan) X-ray diffractometer having Ni-filtered Cu Kα radiation (λ= 1.5406 Å) with a scan speed of 4° min^{-1} and a scan range of 2 – 80° at 40 kV and 20 mA.

The BET surface area of all the catalysts was determined by N_2 physisorption at liquid N_2 temperature i.e. -196 °C (ASAP 2020 Adsorption unit, M/s. Micromeritics, USA). Before the physisorption analysis, the catalyst samples were degassed under vacuum at 250 °C for 1 h to remove the physisorbed moisture.

Temperature programmed reduction (TPR) of the fresh and spent catalysts were performed on homemade reactor setup. About 50 mg of catalyst was placed in a quartz reactor and pre-treated in Ar flow 100 °C for 2 h. A flow of 5% H_2–Ar mixture gas (60 cm^3 min^{-1}) with a temperature ramping of 10 °C min^{-1} was maintained. The hydrogen consumption was monitored by using a thermal conductivity detector (TCD).

A JEOL JEM 2000EXII transmission electron microscope, operating at 160 and 180 kV used to investigate structural features of catalysts. The specimens were prepared by dispersing the samples in acetone using an ultrasonic bath and evaporating a drop of resultant suspension onto the lacey carbon support grid.

H_2 – Chemisorption using pulse (100µL) titration procedure was carried out at 40 °C on a AUTOSORB-iQ, automated gas sorption analyser (M/s. Quantachrome Instruments, USA) to know the dispersion and metal particle size, metal surface area of the catalyst. Prior to the experiment, the catalyst was reduced at 500 °C for 2 hrs followed by evacuation for 2 hrs.

Catalysis procedure

Catalytic tests were performed at atmospheric pressure in a glass down flow fixed bed reactor (14 mm inner diameter, 200 mm long) loaded with 1 g of catalysts mixed with 1 g of quartz beads. Before the catalytic performance, the catalysts were reduced at 500 °C online for 4 h in H_2 flow (30 ml/min). The feed solution comprising of required molar ratio of levulinic acid and formic acid, was fed at a flow rate of 1 ml/h through the micro purfusor feed pump in a stream of N_2 flow (30 ml/min). The product samples were collected at an outlet of the reactor and analyzed by a gas chromatograph equipped with a flame-ionization detector. In particular, formic acid decomposition to H_2 and CO_2 was analyzed by a gas chromatograph equipped with a thermal conductivity detector. Furthermore, the conversion of formic acid is not considered because formic acid used as a hydrogen source.

Results and discussion

Temperature programmed reduction studies

Metal-support interactions and reducing behavior of supported metal particles were inferred from TPR results (Figure -1), the NA and NHT catalysts showed three reduction

peaks in their TPR profiles. The first reduction peak appeared at lower temperature (i.e. < 400 °C) is due to the reduction of bulk NiO [23], second peak found at above 500 °C is attributed to the reduction of weakly interacted NiO species with the Al_2O_3 support and third reduction peak noticed at T_{max} centered at around 820 °C is due to the reduction of $NiAl_2O_4$ spinel species whose formation is apparent as a result of the strong metal-support interaction [24]. It is known from the literature that the $NiMgO_2$ solid solution is reduced at the higher temperature at around 800 ^oC [25]. So one cannot ignore the formation of $NiMgO_2$ solid solution in NHT catalyst. Hence, the major reduction peak found in the NHT belongs to the reduction of $NiMgO_2$ species. As it can be seen from the Figure-1, the contribution of $NiMgO_2$ is very high compared to $NiAl_2O_4$. The TPR results suggested that the weakly interacted NiO species are the foremost species in the NA catalyst whereas strongly interacted species i.e., $NiMgO_2$ are the major species in the NHT catalyst. On the contrary, two broad reduction peaks were observed in the NM catalyst. The first broad reduction peak noticed at around 500 °C is ascribed to weakly interacted NiO with MgO support [25, 26]. While the second broad peak found at the higher temperature around 800 °C is attributed to the reduction of NiO–MgO ($MgNiO_2$) solid solution [27]. The formation of NiO-MgO solid solution is conceivable in NM and NHT catalyst due to the presence of defect sites in MgO and similar sizes of NiO and MgO [28]. Furthermore, the strong reduction peak at the higher temperature in the case of NHT might be attributed to the substitution of Ni in place of Mg in hydrotalcite. The higher temperature reduction peak could be ascribed to substituted Ni in hydrotalcite structure [29].

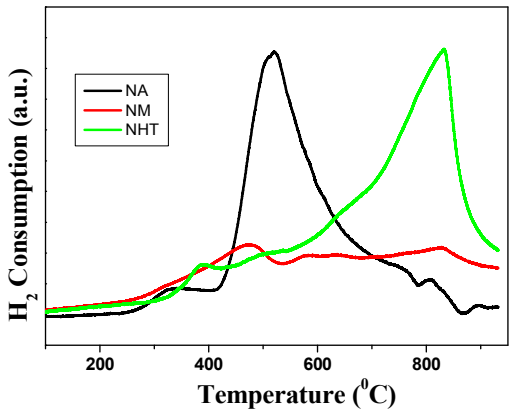

Figure – 1. TPR profiles of all the Ni-based catalysts.

X-ray diffraction studies

Figure-2 represents the reduced XRD patterns of NA, NM and NHT catalysts. The NA catalyst showed the 2θ values at 44.49°, 51.85° and 76.38° which corresponds to the metallic Ni with face centered cubic geometry of the space group Fm3m (225) with cell parameter 3.523 A° (ICDD.No.87-0712). In addition to these peaks, the catalysts, NM and NHT are also showed some 2θ values at 37.04, 62.49, and 78.88º which belong to $NiMgO_2$ (ICDD No.24-0712) or MgO. It is renowned that the XRD patterns of the (Mg, Ni)O (i.e. $NiMgO_2$) phase cubic system, space group Fm3m and parameter a = 4.1922 A^0, has similar structural integrity as that off MgO (cubic system, spatial group Fm3m, parameter a = 4.209 A °) phase [25] so it's hard to assign those peaks belongs to any one of the single phase i.e. $NiMgO_2$ or MgO. The peaks corresponding to hydrotalcite structure was not found in both (calcined and reduced NHT catalysts) catalysts. This could be due to the loss of interlayer anions during the calcination and reduction processes.

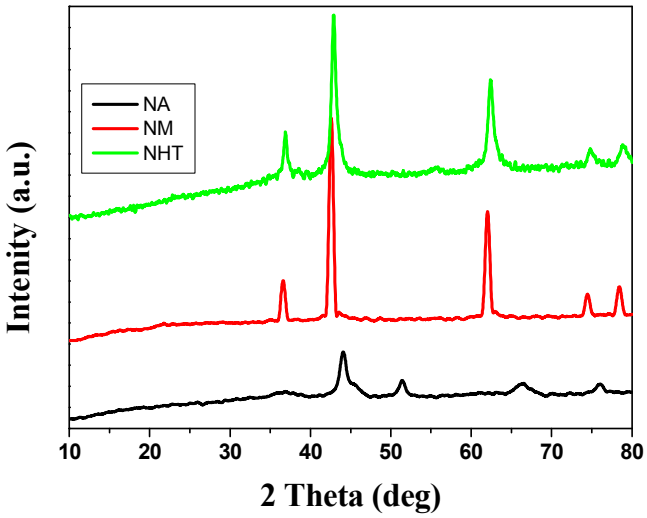

Figure –2. XRD patterns of all the Ni-based catalysts.

Scanning electron microscopy studies

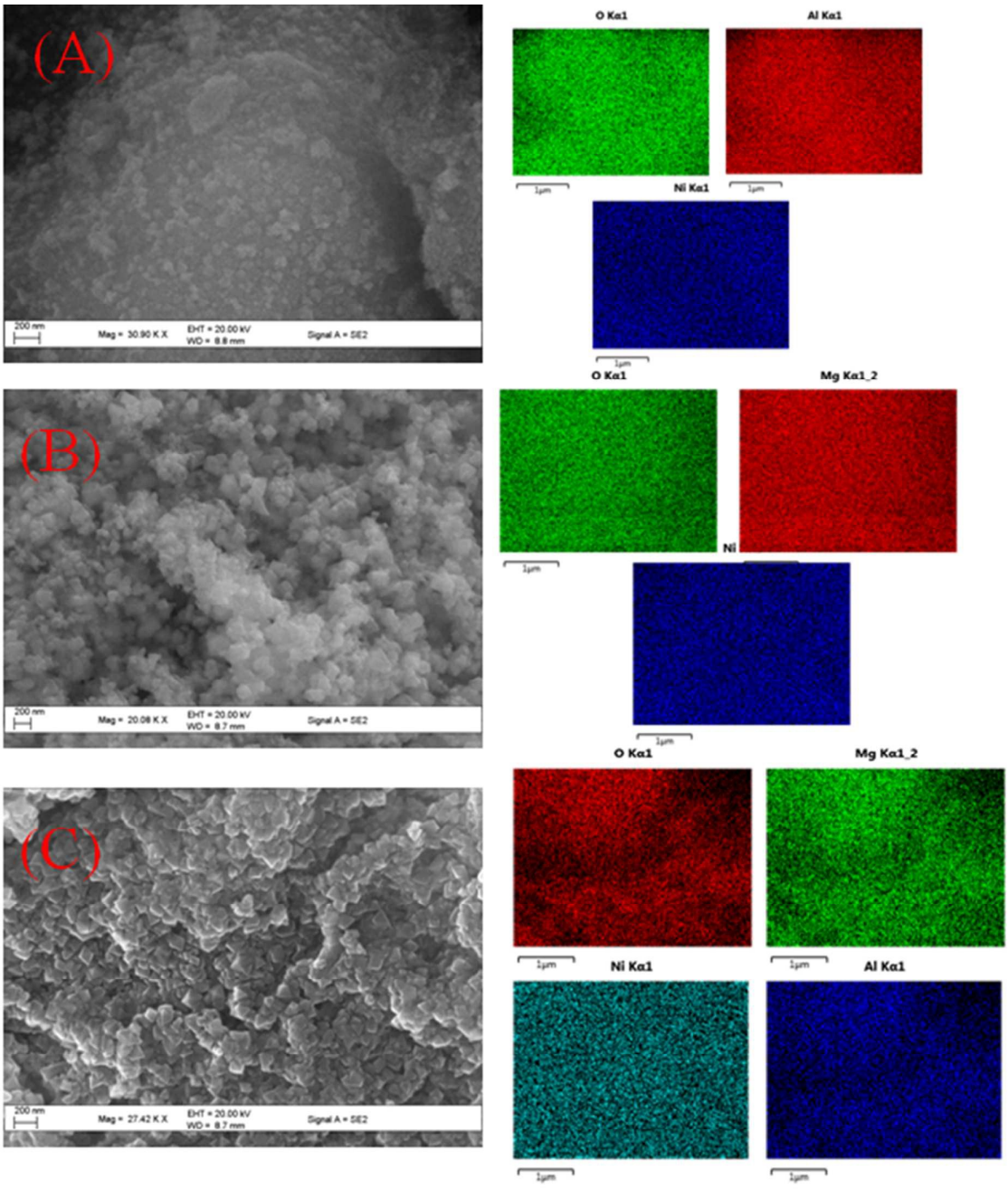

Figure – 3. SEM patterns of all the Ni-based catalysts (A) Ni/Al_2O_3 (B) Ni/MgO and (C) $Ni/MgO\text{-}Al_2O_3$.

Figure- 3(A) clearly shows the presence of Ni (small whitish particles) on Al_2O_3 surface. It can be seen from the Figure-3(B) that Ni particles are uniformly distributed on/in MgO surface by forming a solid solution and hence there is no clear distinction between Ni and MgO. Similar kind of information is noticed in the case of NHT, Figure-3(C), which might be

due to the predominant formation of $NiMgO_2$ solid solution. The results are in line with the TPR results as evidenced from the Figure- 1. Elemental mapping investigations were performed by EDS analysis from various points of the NA, NM and NHT catalysts revealed the respective elements.

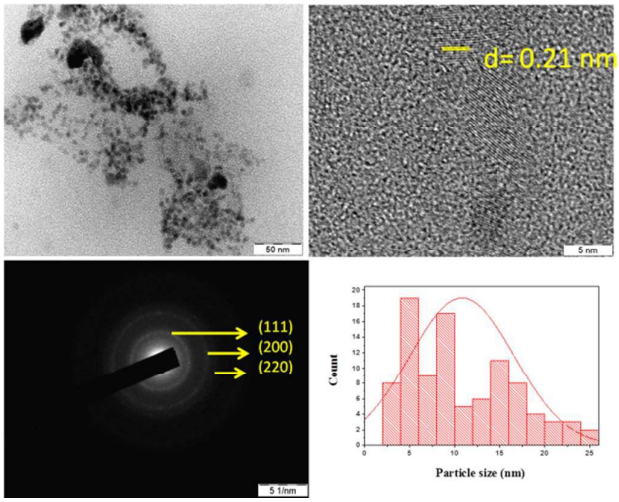

Figure – 4. TEM, HRTEM image, SAED pattern and particle size distribution of NA catalyst.

Besides, from the TEM image of NA, one can conclude that the Ni particles are well dispersed and in a range of 5-15 nm which is fine harmonized with the H_2 chemisorption studies (Table-1). It can be inferred from the HRTEM (Figure-4) that the interplanar distance between the Ni crystals is found to be 0.21 nm which is concomitant with the previous reports [30]. Besides, the SAED pattern of NA catalyst clearly justifies the crystalline nature of Ni as evidenced from the XRD studies (Figure-2).

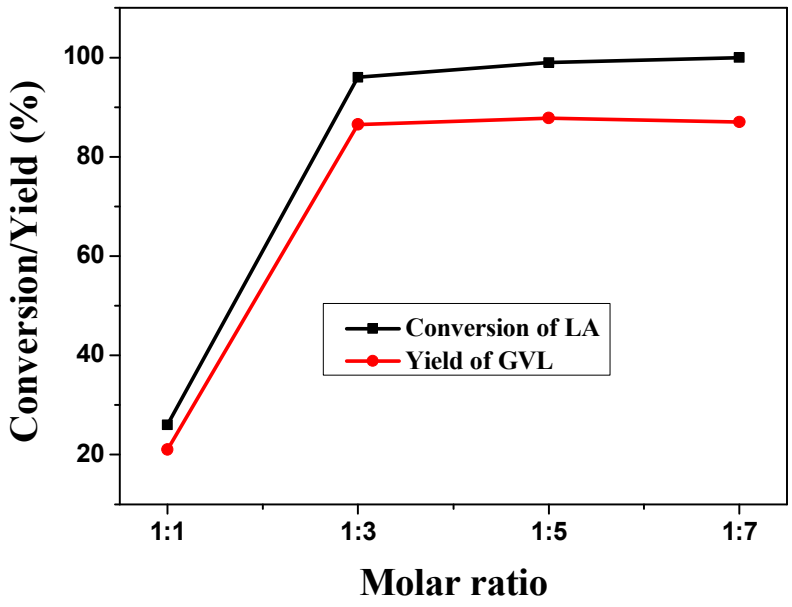

Figure- 5. Influence of LA and FA molar ratio on the LA hydrogenation activity over NA catalyst. Reaction conditions: Weight of the catalyst =1 g, Temperature=250 °C, Pressure=1 atm, carrier gas (N_2) = 1800 ml h^{-1}.

Surprising results were found when we carried out the hydrogenation of levulinic acid using formic acid as a sole hydrogen source. It can be inferred from the Figure- 5 that the influence of LA and FA molar ration on the LA hydrogenation over NA catalyst. The results suggest that the conversion of LA increases as the molar ratio of FA increases. The conversion of levulinic acid is very low (26%) when the molar ratio of LA: FA is 1:1 and it is found to be increased to 96% when the molar ratio of LA: FA is 1:3 and further it reached to 99% when the molar ratio of LA: FA is 1:5. No significant variation in the conversion of LA to GVL is noticed beyond the molar ratio of 1:5. Hence, this optimum parameter (i.e. LA: FA=1:5) is used for the further studies such as catalyst optimization and time on stream. From the Figure-6, it is clear that the NA catalyst showed highest catalytic activity compared to other two catalysts. Lowest conversion is noticed over NHT due to the substitution of Ni in place of Mg as inferred from the TPR profiles (Figure - 1). Furthermore, NM suggesting high catalytic performance similar to NA might be due to the formation of $NiMgO_2$ solid solution which results in promoting the enhanced performance. The highest catalytic activity of NA can be attributed to the largely available weakly interacted NiO species with the Al_2O_3 support which upon reduction yield the high number of Ni metallic species. The catalytic

activity results suggest that the NA is an efficient catalyst for the hydrogenation of LA. Additionally, as it can be inferred from the XRD patterns of reduced catalysts (Figure- 2), the differentiation of Ni in NM and NHT is not possible might be due to the formation of $NiMgO_2$ solid solution (Figure- 2). Furthermore, the XRD patterns and SEM results are in good agreement with the TPR patterns (Figure- 3).

Moreover, we performed the reaction over high surface area materials like zeolite and silica supported Ni catalysts at an optimized reaction conditions. Around 91.5% conversion of levulinic acid was noticed with 67.1% selectivity to GVL over Ni/HZSM-5 catalyst. Interestingly, 25.8% of pentanoic acid was observed which could be due to the cleavage of formed GVL i.e. well know Bronsted acidity of zeolite). In addition, 7% of angelica lactone intermediate was also noticed. On the other hand, 98.2% levulinic acid conversion and 77.1% selectivity to GVL was observed over Ni/SiO_2 catalyst. For the comparison, we also performed the hydrogenation of levulinic acid with external hydrogen and noticed 98.6% levulinic acid conversion and 84% selectivity to GVL over NA catalyst.

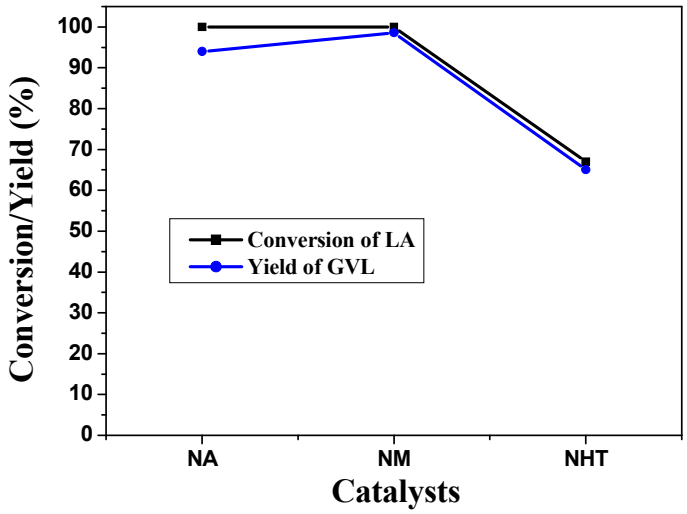

Figure- 6. Variation in the conversion of LA and yield of GVL against all the Ni-based catalysts. Reaction conditions: Weight of the catalyst=1 g, Temperature=250 °C, Pressure=1 atm, carrier gas (N_2) = 1800 ml h^{-1}, FA/LA molar ratio = 5, Feed flow = 1 ml h^{-1}.

To further verify the reasons for the differences in the catalytic activity of all the catalysts, we performed the H_2 pulse chemisorption studies (Table-1) to know the metal surface area, particle size and Ni dispersion on various carriers such as MgO, Al_2O_3, and HT, which influence a lot on the catalytic activity. The chemisorption results indicate that the NA catalyst has a high active metal (Ni) surface area along with lower particle size and high dispersion than the other catalysts.

Catalyst	SA (m^2/g)[a]	Nm (µmoles/g) [b]	AMSA (m^2/g) [b]	d (nm) [b]	D (%) [b]
NA	134	165.9	13.0	15.6	6.5
NM	15	101.9	8.0	25.4	4.0
NHT	18	70.12	5.49	36.9	2.7

Table-1. Physico-chemical properties of all the nickel-based catalysts. [a] BET surface area determined from N_2 gas adsorption, [b] Calculated by H_2-pulse chemisorption.

As evidenced from the H_2 pulse chemisorption and TEM, the greater number of surface Ni species with lower particle size and high dispersion of Ni stands the NA as a promising catalyst for hydrogenation of LA among the other catalytic systems. A large number of Ni surface species with smaller particle size can be conceivable due to the high content of weakly interacted NiO species with Al_2O_3 in the NA catalyst found in its TPR profile, and all these species are reducible in the catalyst reduction temperature i.e. 500 °C used in the present investigation.

As aforementioned that the all the three catalysts are efficient for the hydrogenation of levulinic acid in the absence of an external hydrogen. In addition, to find out the stability of all the catalysts, time on stream analysis was carried out for a period of 10 h at an optimized reaction conditions (FA/LA molar ratio = 5, Feed flow = 1 ml h^{-1}, Temperature 250 °C, 1 atmosphere). The outcome of the results is illustrated in Figure- 7A. Although, all the catalysts showed decreased trend in the formation of γ- valerolactone, the drastic decline in the yield of GVL is seen in NM and NHT catalysts. Whereas the gradual decline in the yield of GVL can be observed during the time on stream analysis over NA catalysts; this might be due to an accumulation of carbon species on the surface of the catalyst. While, the presence of the MgO in NM and NHT might be the responsible for the fast catalyst

deactivation during the time on stream analysis over this catalysts, which can be due to the possible transition of a brucite-periclase structure of MgO which could occur whenever water as a one of the by-product in the reaction [31]. To acquire apparent distinction of the activity during the time on stream, we further performed the co-feeding of water along with Levulinic acid, and formic acid over all the catalytic systems. The results (Figure-7B) obtained from the co-feeding of water along with levulinic acid and formic acid (1:1:5 molar ratio of H_2O: FA:LA) substantiates a decrease in the catalytic performance. The phenomenon of drastic decrease of catalytic performance during the time on stream over NM and NHT catalysts presumably due to poisoning effect of water rather than the coke (as evidenced by the TPR patterns of spent catalysts). Although the coke formation is common in all the catalytic systems (as evidenced from the TPR of spent catalysts), the drastic decrease of catalytic performance certainly due to water poisoning. The selectivity to GVL over NA catalyst was a bit lower (94%) up to 3 h after that the selectivity remains complete, i.e., 100%. While in the case of NM and NHT catalysts the selectivity always cent percentage. Though the selectivity is almost cent percentage but the drastic decrease in conversion was noticed over NM and NHT catalysts presumably due to the poisoning of water.

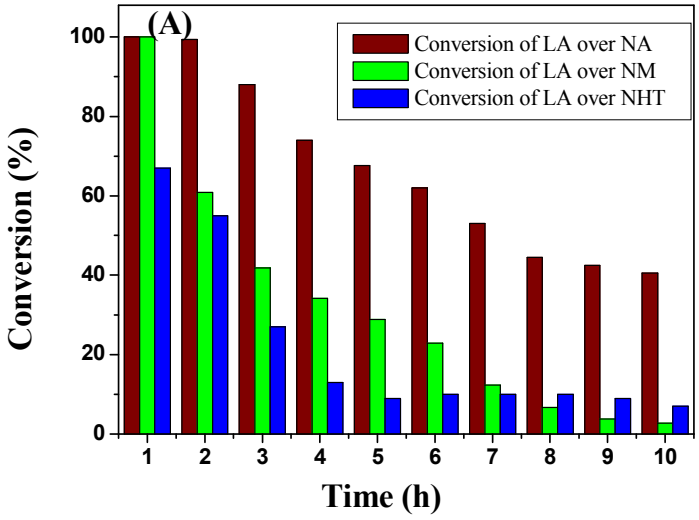

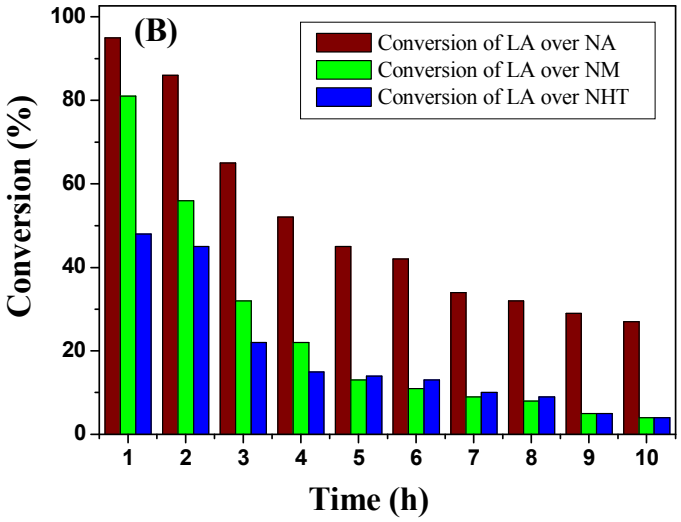

Figure- 7. Influence of time-on-stream over various catalysts at 250 °C. Reaction Conditions: Weight of the catalyst = 1 g, Temperature = 250 °C, Pressure = 1 atm, carrier gas (N_2) = 1800 ml h^{-1}, HCOOH/LA molar ratio = 5, Feed flow = 1 ml h^{-1}. (A) without co-feeding of water (B) with co-feeding of water.

From the time-on-stream studies, one can understand that the catalyst deactivation can be occurred either by the accumulation of carbon species on the catalyst surface or water liberated [32] during the course of the reaction. It is well known that the accumulation of carbon species occurs at the catalyst surface through the condensation of reaction intermediates [2, 25]. In order to find out reasons for catalyst deactivation, we have performed the temperature programmed reduction (TPR) studies for spent catalysts and profiles shown in Figure-8. It is well known in the literature [25, 33] that the accumulated carbon species on the catalyst surface undergo hydrogenation and form methane with the negative signals in the TPR studies of spent catalysts. In the present work, we found the negative signals for all the three catalysts. As a result of the hydrogenation of condensed reaction intermediate such as angelica lactone, on the catalyst surface during the time on-stream analysis. These results suggest that the catalysts deactivation is majorly due to the condensation of reaction intermediates on the catalyst surface. But one cannot ignore the negative effect of water whenever the presence of MgO as a support [25]. the co-feeding of water along with the levulinic acid and formic acid studies showed the drastic decrease in catalytic performance of NM and NHT catalysts. Hence, the drastic decrease in activity during the time on stream over Ni/MgO and Ni/Hydrotalcite catalysts were attributed both

the water produced during the reaction and the coke formation through the condensation of reaction intermediates.

From the bibliographic standpoint, the levulinic acid hydrogenation has been operated in two pathways [2]. In path-1, LA undergoes dehydration over Bronsted acid sites yield angelica lactone (α, β) which upon undergo hydrogenation over metallic sites to form γ-valerolactone [2]. In path-2, hydrogenation of levulinic acid occur over metallic sites produce 4-hydroxy levulinic acid which upon inevitably undergoes dehydration over Bronsted acid sites to form γ-valerolactone [6]. In the present investigation, we observed the formation of angelica lactone as an intermediate in our reaction mixture (as evidenced from GC-MS). It suggests that the hydrogenation of LA with formic acid proceeds through path-1. It indicates that the formic acid not only act as a hydrogen source it can also acts as an acid catalyst which is well established in the earlier literature [31].

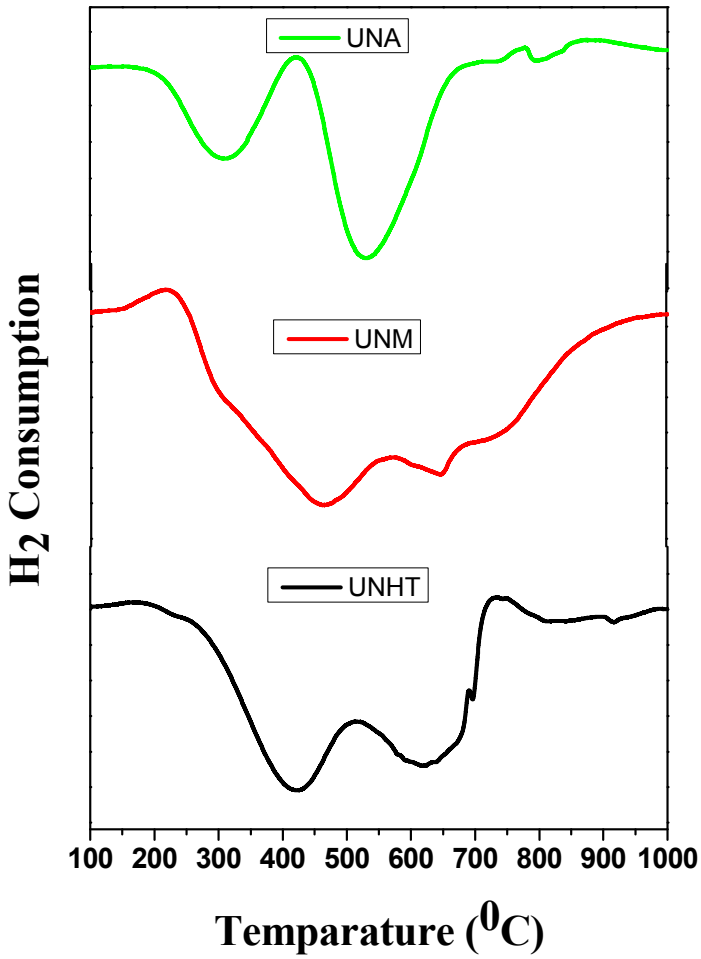

Figure- 8. TPR patterns of spent catalysts.

Conclusions

In summary, we have developed a catalytic system for the efficient conversion of biomass-derived levulinic acid to γ- valerolactone in the absence of external hydrogen source. The generation of largely available weakly interacted NiO species with Al_2O_3 support results the higher number of Ni metallic species with smaller sizes having high dispersion makes the NA as a promising catalytic system for the hydrogenation of levulinic acid with formic acid as hydrogen source than the other catalytic systems. NA catalyst deactivates slowly compared to NM and NHT. Whereas, the presence of MgO in NM and NHT may undergo brucite – periclase transition with the water formed during the hydrogenation of levulinic acid is the major reason for drastic deactivation of these catalytic systems along with coke formation clearly noticed in the study of co-feeding effect of water. Therefore, one can understand that the catalytic systems having MgO as one of the components is not suitable for the reactions in which one of the products is water.

Acknowledgments

One of the authors, VM is grateful to the Council of Scientific and Industrial Research, New Delhi, India for the facilities and financial support.

References

[1]. R. Saxena, D. Adhikari, H. Goyal, *Renewable and Sustainable Energy Reviews*, 2009,**13**, 167-178.

[2]. V.Mohan, C. Raghavendra, C.V. Pramod, B.David Raju, K. S. Rama Rao, *RSC Adv* , 2014,**4**,9660-9668.

[3]. L.E. Manzer, *Appl. Catal. A:Gen*, 2004,**272**, 249-256.

[4]. I. T. Horváth, *Green Chem*., 2008, **10**, 1024-1028.

[5]. D. R. Dodds, R. A. Gross, *Science,* 2007,**318**, 1250-1251.

[6]. D. M. Alonso, S. G. Wettstein, J. A. Dumesic, *Green Chem.*, 2013, **15**, 584-595.

[7]. X. Tang, X. Zeng, Z. Li, L. Hu, Y. Sun, S. Liu , T. Lei , L. Lin, *Renewable and Sustainable Energy Reviews*, 2014, **40**, 608–620.

[8]. V. Mohan, V. Venkateshwarlu, C.V. Pramod, B. D. Raju, K. S. R. Rao, *Catal. Sci. Technol*, 2014,**4**,1253-1258.

[9]. V. Mohan, B. D. Raju, K. S. R. Rao, *J. Catal. Catal*. 2015, **2(2)**, 33-38.

[10] M. Varkolu, V. Velpula, S. Ganji, D. R. Burri, S. R. R. Kamaraju*, RSC Adv*, 2015, **5**, 57201-57210.

[11] V. Mohan, B. D. Raju, K. S. R. Rao, Proceedings of International Conference on New Dimensions in Chemistry & Chemical Technologies-Applications in Pharma Industry (NDCT-2014), Spectrum Publishers, **2014**, 94–96, ISBN 978-93-82829-90-4.

[12] V. Mohan, Thesis submitted to Osmania University, 2014.

[13]. E. Iglesia, M. Boudart*, J. Catal*, 1983, **84,**204-213.

[14]. E. Iglesia, M. Boudart, *J. Catal,* 1983, **84,**214-223.

[15]. E. Iglesia, M. Boudart, *J. Catal*, 1983, **84,**224-238.

[16]. A. M. Hengne, A. V. Malawadkar, N. S. Biradar, C. V. Rode, *RSC Adv*., 2014, **4**, 9730 - 9736.

[17]. R. J. Haan, J.-P. Lange, L. Petrus, C. J. M. Petrus-Hoogenbosch, US patent 2007/ 0208183 A1, Shell Oil Company (2007).

[18] L. Deng, J. Li, D. M. Lai, Y. Fu, Q. X. Guo, *Angew. Chem. Int. Ed*, 2009, **48**, 6529-6532.

[19] X. L. Du, L. He, S. Zhao, Y. M. Liu, Y. Cao, H. Y. He, K. N. Fan, *Angew. Chem. Int. Ed,* 2011, **50**, 7815-7819.

[20] P. P. Upare, M. G. Jeong, Y.K. Hwang, D. H. Kim, Y. D. Kim, D. W. Hwang, U. H. Lee, J. S. Chang, *Appl Catal A Gen,* 2015, **491**, 127-135.

[21]. P. Seetharamulu, V. S. Kumar, A. H. Padmasri, B. D. Raju, K. S. R. Rao, *J. Mol. Catal. A: Chemical,* 2007, **263**, 253-258.

[22]. C. V. Pramod, M. Suresh, V. Mohan, B. Sridevi, B. D. Raju, K. S. R. Rao, *Current Catalysis,* 2012, **1**,140-148.

[23]. T. Wu, Q. Yan, H. Wan, *J. Mol. Catal. A: Chem,* 2005, **226**, 41-48.

[24]. H. V. Fajardo, A. O. Martins, R. M. Almeida, L. K. Noda, L. F. D. Probst, N. L. V. Carreno, A. Valentini, *Mater. Lett*, 2005, **59**, 3963-3967.

[25]. V. Mohan, C.V. Pramod, M. Suresh, K. Hari Prasad Reddy, B. David Raju, K. S. Rama Rao, *Catal Comm*, 2012,**18**,89-92.

[26]. S. Tang, J. Lin, K. L. Tan, *Catal. Lett,* 1998, **51**,169-175.

[27]. T. Furusawa, A. Tsutsumi, *Appl. Catal. A,* 2005, **278**, 207-212.

[28]. A.V. Matveev, K.M. Neyman, I.V. Yudano, N. Rosch, *Surface Science*, 1999, **426**, 123-139.

[29]. K.Y. Koo, H.S. Roh, U.H. Jung, D.J. Seo, Y.S. Seo, W.L. Yoon, *Catal.Today*, 2009, **146**, 166-171.

[30]. Z. Jiang, J. Xie, D. Jiang, X. Wei, M. Chen, *CrystEngComm*, 2013, **15**, 560-569.

[31]. P.A. Son, S. Nishimura, K. Ebitani, *RSC Adv*, 2014, **4**, 10525-10530.

[32]. J. P. Lange, L. Petrus, D. B. P. J. Van, H. K. L. Von, WO2006067171A, 2006.

[33]. S. Chandra Shekar, J. Krishna Murthy, P. Kanta Rao, K. S. Rama Rao, *J. Mol. Catal. A: Chem,* 2003,**191**, 45–49.

Graphical abstract

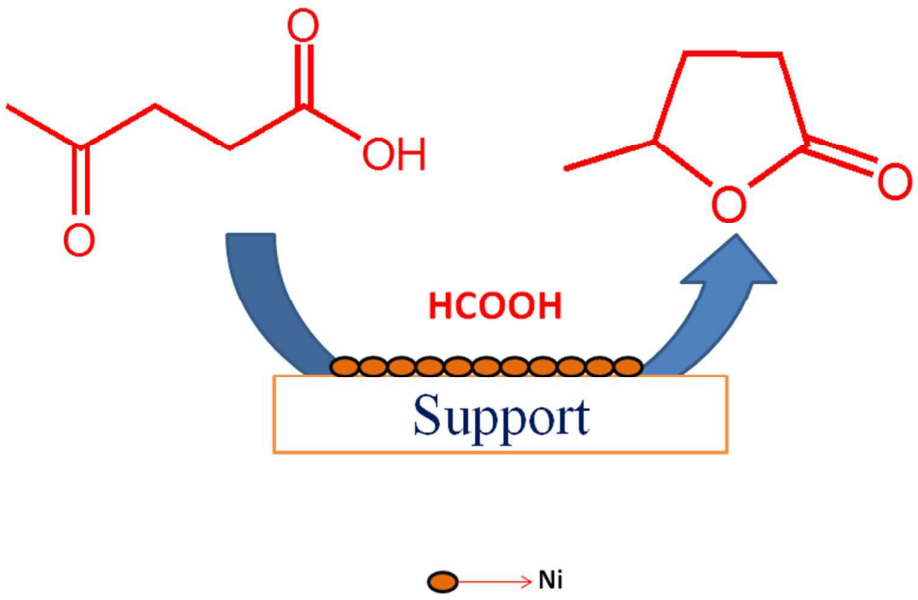

Efficient route for the transformation of levulinic acid without external hydrogen source in continuous process over supported Ni catalysts.